MJSAT

Malaysian Journal of Science and Advanced Technology

journal homepage: https://mjsat.com.my/

Chemically Reactive Unsteady Flow of Casson Fluid over a Stretching Surface

Md. Maruf Hasan *[1], and M Enamul Karim [1]

[1]*Department of Mathematics, Comilla University, Cumilla-3506, Bangladesh.*

KEYWORDS

Chemical Reaction
Casson Fluid
Unsteadiness Parameter

ARTICLE HISTORY

Received 26 March 2025
Received in revised form 1 June 2025
Accepted 12 June 2025
Available online 14 June 2025

ABSTRACT

This study aims to investigate the unsteady flow behaviour of Casson fluid over a stretching surface in the presence of a magnetic field. The effects of magnetic field, Casson parameter and chemical reaction are also accounted for in this model. A Casson non-Newtonian constitutive model is utilized to describe the fluid transport. By employing appropriate similarity transformations, the model equations are reformulated as ordinary differential equations. Then the reduced differential equations are solved numerically using the Nachtsheim-Swigert shooting technique along with a sixth-order Runge-Kutta method. The graphical representation illustrates the influence of key physical parameters on flow characteristics. It is indicated that fluid velocity declines with a rise in the unsteadiness parameter and temperature significantly decreases due to this unsteadiness. Moreover, increasing chemical reaction parameter diminishes both velocity and concentration field. Again to validate the accuracy of the developed code, the results are compared with those from earlier research, demonstrating good agreement.

1. INTRODUCTION

A Newtonian fluid is defined as a fluid whose viscosity remains unchanged when shear stress is applied at a constant temperature. This indicates a direct linear relation between viscosity and shear stress for these fluids. Conversely, non-Newtonian fluids exhibit viscosity that is influenced by factors beyond temperature. In these cases, the viscosity alters in response to applied shear stress. The connection between stress and shear rate in these fluids can differ and may even change over time. The nonlinear connection between stress and shear rate in these fluids complicates the formulation of a single constitutive equation that can explain all their characteristics. As a result, multiple models for non-Newtonian fluids have been developed, each based on different physical characteristics [1]. Among these models, the Casson fluid is the most widely recognized [2].

The Casson fluid is defined as a liquid that exhibits shear-thinning behaviour. At a shear rate of zero, it is deemed to have infinite viscosity, while at an infinitely high shear rate, it is characterized by zero viscosity. This fluid functions in a way comparable to elastic solids and its constitutive equation includes a yield shear stress. Numerous experiments conducted on blood indicate that its behaviour aligns closely with that of a Casson fluid [3]. Specifically, the Casson fluid model provides a more precise representation of blood flow characteristics, particularly at low shear rates and within narrow blood vessels [4]. The Casson fluid model has proven to be relevant in the development of blood oxygenators and hemodialysis systems.

The concept of the stretching sheet problem was first introduced by McCormack and Crane in 1973 [5]. This problem has become important in various engineering applications and industrial sectors, including fluid dynamics, magnetohydrodynamic flows, porous situation and the study of heat. The combined heat and mass movement represents a critical challenge in fluid dynamics. This phenomenon is applicable in various engineering and industrial processes [6].

The equations governing the boundary layer for unsteady flow were elucidated by [7]. The dynamics of flow and heat transfer in a thick environment were analyzed by [8]. MHD flow along a vertical plate was studied by [9]. However, they did not consider Soret effect. Dufour impact in conjunction with MHD flow was addressed by [10]. A study by [11]

*Corresponding author:
E-mail address: Md. Maruf Hasan < marufek@gmail.com >.
https://doi.org/10.56532/mjsat.v5i2.509
2785-8901/

emphasized exponential profiles for surface flow fields. The micropolar fluid flow across an exponentially varying surface was discussed by [12]. The slip impact on stretching sheet was explained by [13]. Then the non-steady magnetohydrodynamic flow past a vertical plate was examined by [14]. Another study conducted by [15] focused on convective movement and heat transfer along perpendicular plate.

Due to the common presence of non-Newtonian fluid in different areas, no considerable efforts have yet been made to examine the unsteady flow of Casson fluid. Previous research has made significant progress in understanding the behavior of Newtonian fluids and chemical reactions separately. Yet, the combined influences of Casson model, unsteadiness and chemical reaction phenomena have not been thoroughly investigated. Moreover, a number of researchers disregard the non-Newtonian characteristics of Casson fluids, which are essential for the accurate modeling of materials such as blood and ink.This study intends to fill this void in the literature. It focuses on the chemically reactive unsteady flow of Casson fluid over a stretching surface in presence of magnetic field. Numerical methods are employed to solve the dimensionless equations and the impacts of different physical factors on flow characteristics are illustrated and examined through graphical representation.

2. CASSON FLUID MODEL

The Casson rheological model [16, 17] is given by

$$\tau_{ij} = 2\left(\mu_b + \frac{P_y}{\sqrt{2\pi}}\right)e_{ij} \tag{1}$$

where

$$e_{ij} = \frac{1}{2}\left(\frac{\partial v_i}{\partial x_j} + \frac{\partial v_j}{\partial y_i}\right) \tag{2}$$

and $i, j = x, y$. The rate of strain tensor is

$$e_{ij} = \begin{pmatrix} e_{xx} & e_{xy} \\ e_{yx} & e_{yy} \end{pmatrix} \tag{3}$$

Again

$$\tau_{ij} = 2\mu_b\left(1 + \frac{P_y}{\mu_b\sqrt{2\pi}}\right)e_{ij} = 2\mu_b\left(1 + \frac{1}{\beta}\right)e_{ij} \tag{4}$$

Then stress tensor is

$$\tau_{ij} = \begin{pmatrix} \tau_{xx} & \tau_{xy} \\ \tau_{yx} & \tau_{yy} \end{pmatrix} = \begin{pmatrix} 2\mu_b\left(1 + \frac{1}{\beta}\right)\frac{\partial u}{\partial x} & \mu_b\left(1 + \frac{1}{\beta}\right)\left(\frac{\partial u}{\partial y} + \frac{\partial v}{\partial x}\right) \\ \mu_b\left(1 + \frac{1}{\beta}\right)\left(\frac{\partial v}{\partial x} + \frac{\partial u}{\partial y}\right) & 2\mu_b\left(1 + \frac{1}{\beta}\right)\frac{\partial v}{\partial y} \end{pmatrix} \tag{5}$$

Here μ_b be the plastic dynamic viscosity, P_y be yield stress, β be Casson fluid parameter. Again the yield stress $P_y = 0$ for Newtonian case.

3. MATHEMATICAL REPRESENTATION

Two-dimensional unsteady flow viscous Casson fluid over a stretching surface affected by a chemical reaction is considered here. The fluid is electrically conducting and incompressible. The x-axis is aligned with surface direction and y-axis is perpendicular to it. A uniform magnetic field of strength B_0 is applied in y-direction. Our interest lies in the study of the effects of the applied magnetic field on fluid flow. In this scenario, the magnetic Reynolds number is considerably less than one. Thus the induced magnetic field's influence is viewed as minor relative to that of the applied magnetic field. It is also considered that T_w and C_w are constant surface temperature and surface concentration and T_∞ and C_∞ are at a distance from the surface. Then the main equations for the unsteady flow of Casson fluid are

$$\frac{\partial u}{\partial x} + \frac{\partial v}{\partial y} = 0 \tag{6}$$

$$\frac{\partial u}{\partial t} + u\frac{\partial u}{\partial x} + v\frac{\partial u}{\partial y} = \upsilon\left(1 + \frac{1}{\beta}\right)\frac{\partial^2 u}{\partial y^2} + g\beta_T(T - T_\infty) + g\beta_C(C - C_\infty) - \frac{\sigma B_0^2}{\rho}u \tag{7}$$

$$\frac{\partial T}{\partial t} + u\frac{\partial T}{\partial x} + v\frac{\partial T}{\partial y} = \frac{\kappa}{\rho C_p}\frac{\partial^2 T}{\partial y^2} + \frac{Q_0}{\rho C_p}(T - T_\infty) \tag{8}$$

$$\frac{\partial C}{\partial t} + u\frac{\partial C}{\partial x} + v\frac{\partial C}{\partial y} = D_m\frac{\partial^2 C}{\partial y^2} - K(C - C_\infty) \tag{9}$$

The corresponding boundary conditions are

$$\left.\begin{array}{ll} u = u_w, v = -v_0(x), T = T_w, \mathrm{C} = \mathrm{C_w} & \text{at } y = 0 \\ u = 0, \quad T = \mathrm{T_\infty}, \mathrm{C} = \mathrm{C_\infty} & \text{at } y \to \infty \end{array}\right\} \tag{10}$$

where u and v be the velocity components in x and y directions respectively, $\upsilon = \frac{\mu_b}{\rho}$ is kinematic viscosity for Casson fluid, g is acceleration due to gravity, β_T and β_C are volumetric co-efficient of thermal and concentration expansions, ρ is fluid density, C_p is specific heat, κ is thermal conductivity, σ is electric conductivity, Q_0 is volumetric rate of heat generation, D_m is chemical molecular diffusivity, K is reaction rate, u_w is the tangential velocity, v_0 represents the velocity component at the wall, with a positive value indicating the presence of suction.

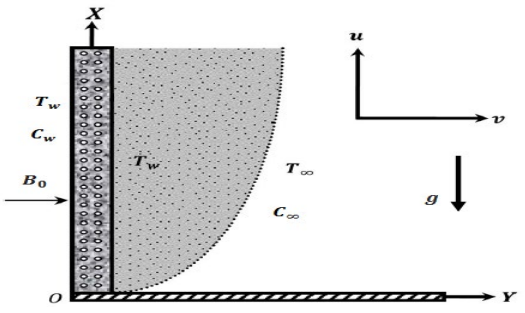

Fig. 1. Schematic of flow configuration

By introducing the following similarity variables, it is possible to convert the governing equations (6) to (9) into a dimensionless form.

$$\left.\begin{aligned} u = \frac{cx}{1-\lambda t} f'(\eta), v = -\sqrt{\frac{c\vartheta}{1-\lambda t}} f(\eta), \eta = y\sqrt{\frac{c}{\vartheta(1-\lambda t)}} \\ \psi = \sqrt{\frac{c\vartheta}{1-\lambda t}}\, xf(\eta), \theta(\eta) = \frac{T-T_\infty}{T_w - T_\infty}, \phi(\eta) = \frac{C-C_\infty}{C_w - C_\infty} \end{aligned}\right\} \quad (11)$$

where ψ be the stream function, η be the dimensionless distance normal to the surface, θ be the dimensionless temperature and ϕ be the dimensionless concentration.

Using equation (11) the above governing equations become

$$\left(1+\frac{1}{\beta}\right) f''' + ff'' - f'^2 + Gr\theta + Gc\phi - Mf' - A\left(f' + \frac{\eta}{2} f''\right) = 0 \quad (12)$$

$$\theta'' + Pr\theta'(f - A\frac{\eta}{2}) + Pr\theta Q = 0 \quad (13)$$

$$\phi'' + Sc\phi'\left(f - A\frac{\eta}{2}\right) - Sc\gamma\phi = 0 \quad (14)$$

The reduced boundary conditions are

$$\left.\begin{aligned} f' = 1, f = f_w, \theta = 1, \phi = 1 \text{ at } \eta = 0 \\ f' = 0, \quad \theta = 0, \phi = 0 \text{ at } \eta \to \infty \end{aligned}\right\} \quad (15)$$

where $A = \frac{\lambda}{c}$ is the unsteadiness parameter, $M = \frac{\sigma B_0^2(1-\lambda t)}{\rho c}$ is the magnetic field parameter, $Gr = \frac{g\beta_T(T_w - T_\infty)(1-\lambda t)^2}{c^2 x}$ is the thermal Grashof number, $Gc = \frac{g\beta_T(T_w - T_\infty)(1-\lambda t)^2}{c^2 x}$ is the Concentration Grashof number, $Pr = \frac{\mu C_p}{k}$ is the Prandtl number, $Q = \frac{Q_0}{\rho C_p c}(1-\lambda t)$ is the heat source parameter, $f_w = -v_w\left(\frac{c\vartheta}{1-\lambda t}\right)^{-1/2}$ is the suction parameter, $Sc = \frac{v}{D_m}$ is the Schmidt number, $\gamma = \frac{k(1-\lambda t)}{c}$ is chemical reaction parameter.

Again the Skin friction coefficient(C_f), local Nusselt number (Nu_x) and Sherwood (Sh_x) number can be written as

$$C_f = Re_x^{-\frac{1}{2}} f''(0),\ Nu_x = -Re_x^{\frac{1}{2}}\theta'(0), Sh_x = -Re_x^{\frac{1}{2}}\phi'(0) \quad (16)$$

where Re_x is the local Reynolds number.

4. MATHEMATICAL COMPUTATION

The numerical solution of the reduced differential equations (12)-(14) under the boundary conditions (15) was achieved through the shooting method namely Nachtsheim-Swigert [18] iteration technique combined with a sixth-order Runge-Kutta iteration scheme. A step size of $\Delta\eta = 0.01$ was employed to ensure a convergence criterion of 10^{-6} throughout the entire duration. The value of η_∞ was determined in each iteration loop using the formula $\eta_\infty = \eta_\infty + \Delta\eta$. The computations were carried out using FORTRAN symbolic software. This method has been widely adopted in recent years for its efficiency in solving highly nonlinear problems. Additionally, a Runge-Kutta algorithm was applied, which incorporated a collocation method involving polynomials of a certain degree, a set of points within the domain known as collocation points and a solution that meets the requirements of the equation at these collocation points.

5. RESULTS AND DISCUSSIONS

This section focuses on the discussion and analysis of velocity distribution, as well as the thermal and mass characteristics for various flow parameters. We know that our body temperature is $T = 310K$ and the value of Prandtl number for human blood is $Pr = 21$ [19]. So Pr is reserved 21 in this study.

5.1 Effect of Unsteadiness Parameter

Figures 2, 3 and 4 illustrate the impact of unsteadiness parameter A on flow fields. As depicted in Figure 2, a raise in A gives a decline in velocity, suggesting a reduction in momentum boundary layer. A comparable trend is observed in the temperature and concentration fields, as demonstrated in Figures 3 and 4.

5.2 Effect of Casson Fluid Parameter

The impact of the Casson fluid parameter β on flow fields is presented in Figures 5, 6 and 7. Figure 5 clearly indicates that as β increases from 0.6 to 1, the velocity field diminishes by roughly 40%. This phenomenon occurs because β is directly related to the plastic dynamic viscosity μ_b , which introduces resistance in the fluid. In contrast, β has a positive effect on the temperature field as sown in Figure 6. Furthermore, the retarding force generated by the plastic dynamic viscosity μ_b leads to an increase in the concentration profiles illustrated in Figure 7.

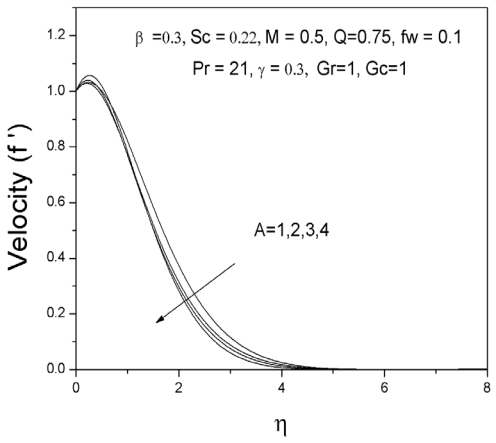

Fig. 2. Velocity profiles for different values of A

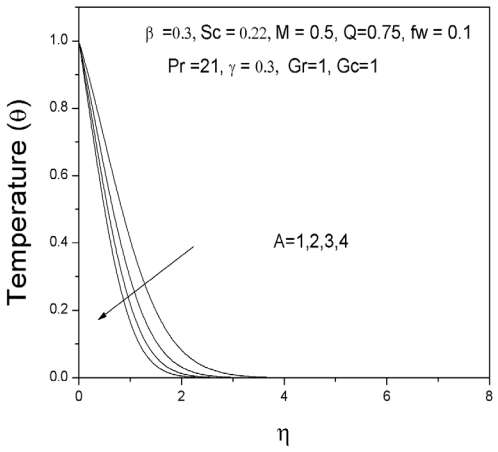

Fig. 3. Temperature profiles for different values of A

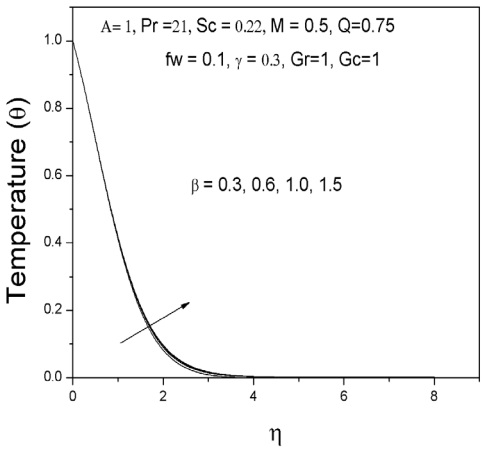

Fig. 6. Temperature profiles for different values of β

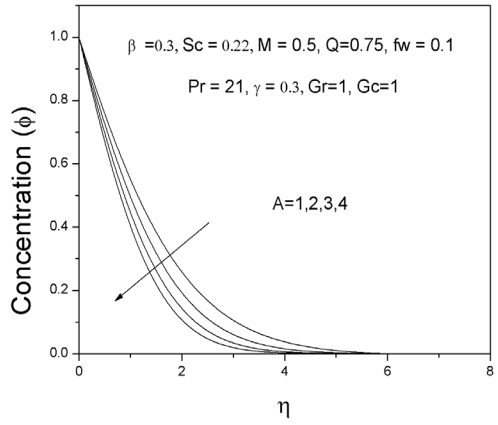

Fig. 4. Concentration profiles for different values of A

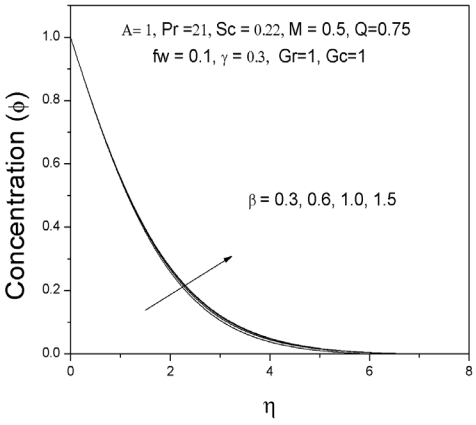

Fig. 7. Concentration profiles for different values of β

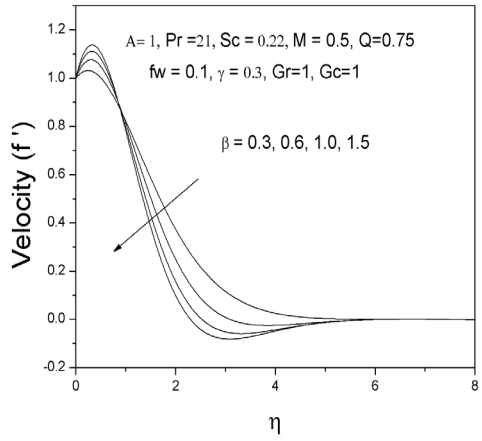

Fig. 5. Velocity profiles for different values of β

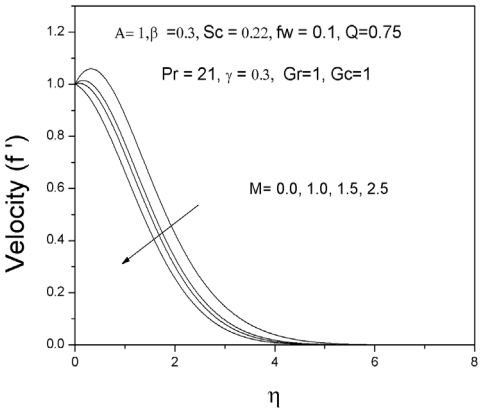

Fig. 8. Velocity profiles for different values of M

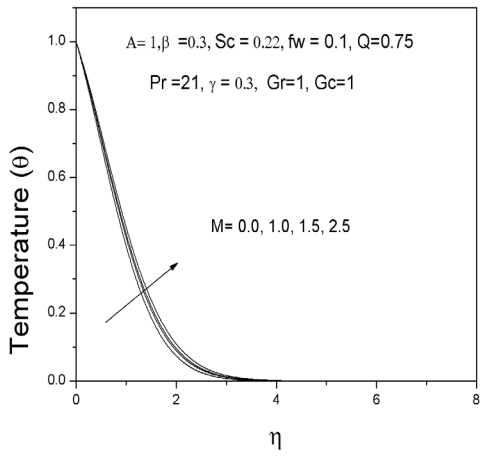

Fig.9. Temperature profiles for different values of M

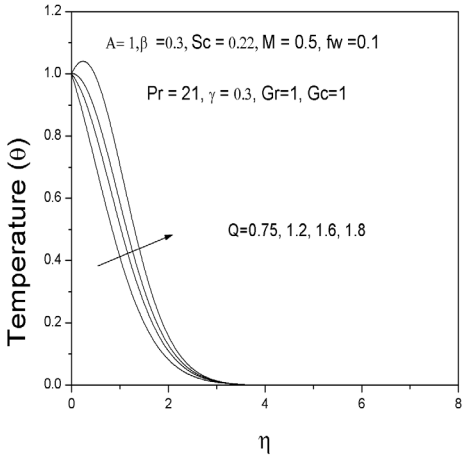

Fig.12. Temperature profiles for different values of Q

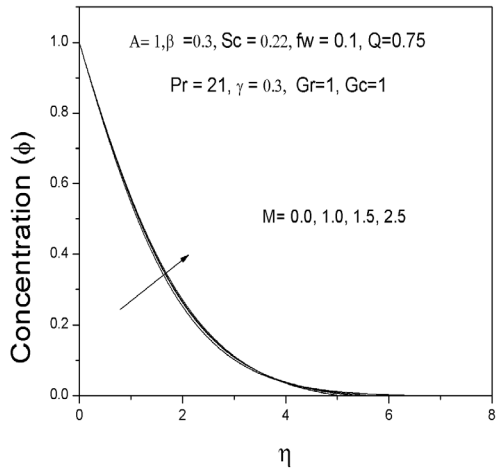

Fig. 10. Concentration profiles for different values of M

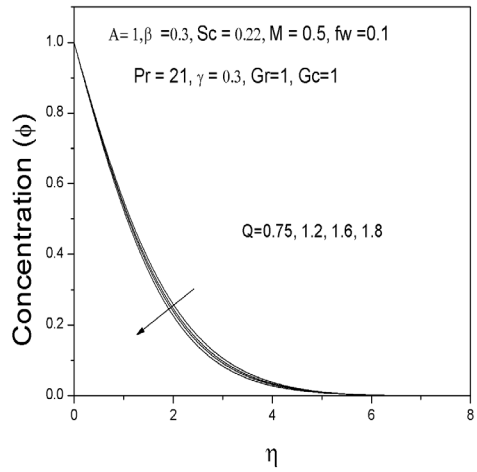

Fig. 13. Concentration profiles for different values of Q

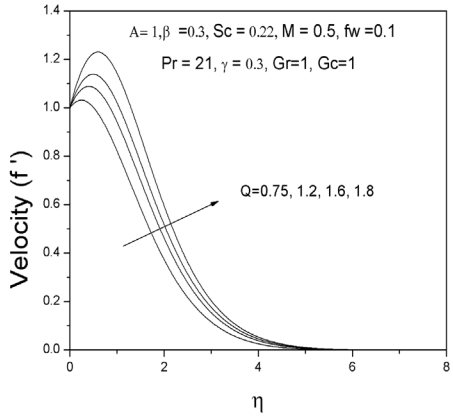

Fig 11. Velocity profiles for different values of Q

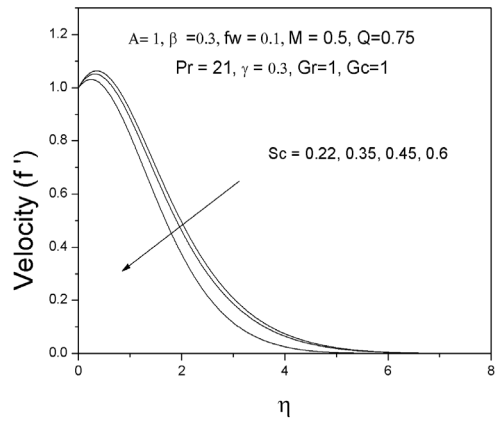

Fig. 14. Velocity profiles for different values of Sc

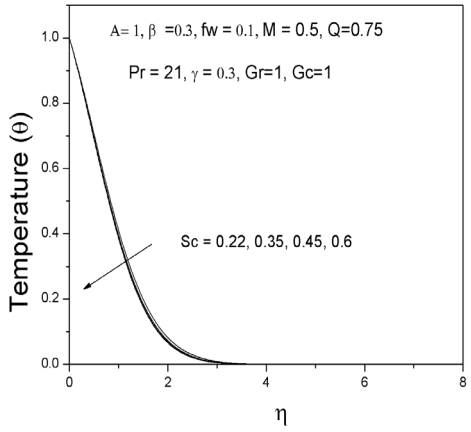

Fig.15. Temperature profiles for different values of Sc

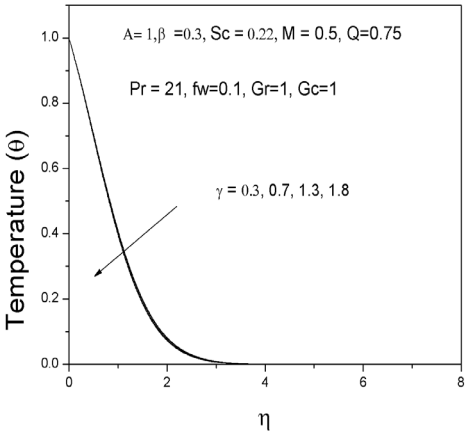

Fig. 18. Temperature profiles for different values of γ

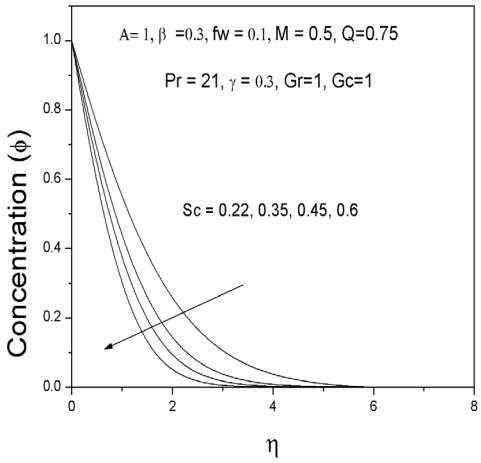

Fig. 16. Concentration profiles for different values of Sc

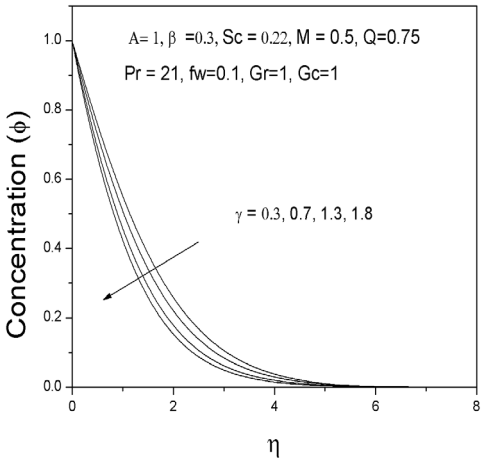

Fig.19. Concentration profiles for different values of γ

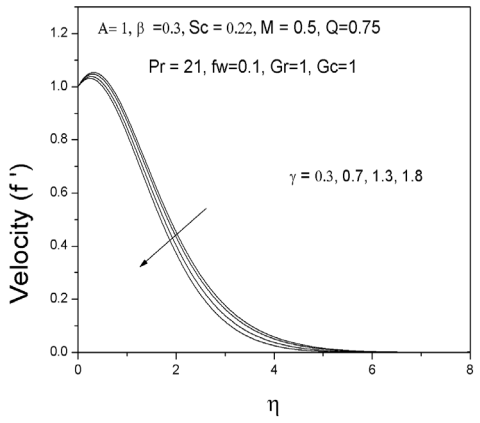

Fig.17. Velocity profiles for different values of γ

5.3 Effect of Magnetic Field Parameter

The impact of the magnetic field parameter M is illustrated in Figures 8, 9 and 10. It is evident that when M increases from 1 to 1.5, the velocity field experiences a reduction of nearly 25%. This reduction occurs because M generates a force within the flow field, referred to as the Lorentz force, which hinders fluid movement. Conversely, Figures 9 and 10 demonstrate an opposite trend for other fields.

5.4 Effect of Heat Source Parameter

In Figures 11, 12 and 13 we present the profiles of velocity, temperature and concentration for some heat source parameter Q. It is understood that the heat generation enhances the buoyancy force, leading to a raise in flow rate and consequently velocity field is elevated by almost 50% when Q increases from 0.75 to 1.6, depicted in Figure 11. Additionally, as Q increases from 0.75 to 1.6, the temperatures undergo a swift rise of nearly 65%. This indicates that during fluid flow, heat generation significantly expands the thickness

of thermal boundary layer. Figure 13 shows that the concentration field diminishes as the heat source parameter increases.

5.5 *Effect of Schmidt Number*

The impact of the Schmidt number Sc on flow characteristics are presented in Figures 14, 15 and 16. It is observed that Schmidt number has a considerable effect on the transport of momentum and mass. Typically, an increase in the Schmidt number affects the relative diffusion rates of both momentum and mass. This phenomenon is frequently associated with variations in the thickness of the momentum and concentration boundary layers. As depicted in Figure 14, when Sc get large the velocity decreases. Furthermore, Figure 15 indicates that Sc positively influences temperature profile. Similarly, Figure 16, reveals a rapid decline of 75% in concentration profile as Sc increases from 0.22 to 0.35.

5.6 *Effect of Chemical Reaction Parameter*

Figures 17, 18 and 19 illustrate the impact of the chemical reaction parameter γ on flow characteristics. Elevating the chemical reaction parameter generally leads to a reduction in both the concentration and velocity distributions. Consequently, the velocity profile tends to flatten, while the concentration of the reacting species diminishes. Figure 17 shows that the velocity profile decreases with higher values of γ. In contrast, Figure 18, reveals that γ reduces the temperature. Figure 19 illustrates that the concentration profile diminishes by nearly 80% as γ rises from 0.3 to 1.8.

6. RESULTS

In order to confirm the precision of the numerical findings, this study is compared with the earlier research conducted by [20]. The values of heat transfer coefficient $[-\theta'(0)]$ have been compared and demonstrate a remarkable level of agreement, as illustrated in Table 1.

Table 1. Comparison of heat transfer co-efficient for some values of Pr $(A = 0, f_w = 0)$

Prandtl Number (Pr)	Heat transfer co-efficient $[-\theta'(0)]$	
	Earlier research conducted by [20]	*Present Study*
1	0.9547	0.9550
2	1.4714	1.4719
3	1.8691	1.8695
5	2.5001	2.5012
10	3.6603	3.6610

7. CONCLUSION

An analysis has been conducted on the chemically reactive unsteady flow of Casson fluid over a stretching surface influenced by a magnetic field. The dimensionless model equations were solved numerically and the obtained results were displayed graphical formats for various values of the physical parameters.

The conclusions drawn from this study are as follows:

a) Large value of unsteadiness parameter gives a decline in velocity and temperature. So this parameter is useful to investigate the effects of time-dependent factors on the fluid's characteristics.

b) Magnetic field parameter reduces the velocity field. This suggests that the magnetic field is able to control the thickening of the viscosity of fluids. Since it diminishes the speed of flow particles, this feature permits the regulation of fluid velocity.

c) A rise in chemical reaction parameters causes a diminish in concentration profiles. This property has multiple applications in industrial cooling, including manufacturing and pharmaceuticals.

Finally we say that the outcomes of this study will provide a reasonably accurate evaluation of several fluid properties concerning the flow of blood in a physiological environment. The findings of this study will be pertinent to blood vessels in the micro-circulatory system. Furthermore, the analysis also holds significance in industries, where it is frequently necessary to evaluate the flow characteristics of different types of fluids moving through porous frameworks. In addition, the current study will be beneficial in determining the accuracy of future three-dimensional experimental studies that are more complex and may include a greater variety of physical parameters, including radiation, Dufour number and Soret number.

REFERENCES

[1] N. T. M. Eldabe NTM, G. Saddeck, and A. F. El-Sayed, "Heat transfer of MHD non-Newtonian Casson fluid flow between two rotating cylinders," Mechanics and Mechanical Engineering, vol. 5, no. 2, pp. 237-251, 2001. doi: https://doi.org/10.4236/am.2024.158034

[2] S. Nadeem, R. U. Haq, and C. Lee, "MHD flow of a Casson fluid over an exponentially shrinking sheet," Scientia Iranica, vol. 19, no. 6, pp. 1550-1553, 2012. doi: https://doi.org/10.1016/j.scient.2012.10.021

[3] N. Casson, "Flow equation for pigment-oil suspensions of the printing ink-type," Rheology of disperse systems, Pergamon Press, Oxford, pp. 84-104, 1959.

[4] R. K. Dash, K. N. Mehta, and G. Jayaraman, "Casson fluid flow in a pipe filled with a homogeneous porous medium," International Journal of Engineering Science, vol. 34, no. 10, pp. 1145-1156, 1996. doi: https://doi.org/10.1016/0020-7225(96)00012-2

[5] P.D. McCormack and L. Crane, "Physics of Fluid Dynamics", New York, Academic Press, 1973.

[6] T. Hayat, M. Sajid, and I. Pop, "Three-dimensional flow over a stretching surface in a viscoelastic fluid," Nonlinear Analysis: Real World Applications, vol. 9, no.4, pp. 1811-1822, 2008. doi: https://dx.doi.org/10.1016/j.nonrwa.2007.05.010

[7] E. M. A. Elbashbeshy, and M. A. A. Bazid, "Heat transfer over an unsteady stretching surface," Heat and mass transfer, vol.41, no. 1, pp. 1-4, 2004. doi: https://doi.org/10.1007/s00231-004-0520-x

[8] S. Sharidan, M. Mahmood, and I. Pop, "Similarity solutions for the unsteady boundary layer flow and heat transfer due to a stretching sheet," Applied Mechanics and Engineering, vol. 11, no. 3, pp. 647, 2006.doi: https://www.researchgate.net/publication/266493374

[9] P. R. Sharma, and G. Singh, "Unsteady MHD free convective flow and heat transfer along a vertical porous plate with variable suction and internal heat generation," International Journal of Applied Mathematics and Mechanics, vol. 4, no. 5, pp. 1-8, 2008. doi: https://citeseerx.ist.psu.edu/document?repid=rep1&type=pdf&doi=207ad262ac07e64dc8d30421b64a23b036b18671.

[10] M. S. Alam, M. M. Rahman, and M. A. Samad, "Dufour and Soret effects on unsteady MHD free convection and mass transfer flow past a vertical porous plate in a porous medium," Nonlinear Analysis: Modelling and Control, vol. 11, no. 3, pp. 217-226, 2006. doi: https://doi.org/10.15388/NA.2006.11.3.14743

[11] H. Bararnia, M. Gorji, G. Domairry, and A. R. Ghotbi, "An analytical study of boundary layer flows on a continuous stretching surface," Acta applicandae mathematicae, vol. 106, pp.125-133, 2009. link: https://link.springer.com/article/10.1007/s10440-008-9286-3

[12] M. A. El-Aziz, "Viscous dissipation effect on mixed convection flow of a micropolar fluid over an exponentially sheet," Can. J. Phys., vol.87, pp. 359-368, 2009. doi: http://dx.doi.org/10.1139/P09-047

[13] K. Bhattacharyya, S. Mukhopadhyay, and G. C. Layek, "Slip effects on an unsteady boundary layer stagnation-point flow and heat transfer towards a stretching sheet," Chinese Physics Letters, vol. 28, no.9, pp. 094702, 2011. doi: https://doi.org/10.1088/0256-307X/28/9/094702

[14] D. Iranian, P. Loganathan, and P. Ganesan, "Unsteady MHD natural convective flow over vertical plate in thermally stratified media with variable viscosity and thermal conductivity," International Journal of Computer Applications, vol. 121, no. 3, pp.18-24, 2015. doi: https://citeseerx.ist.psu.edu/document?repid=rep1&type=pdf&doi=a145dd7e73c429a7f600611d574eaa1dc193e324

[15] N. C. Mathanti, and P. Gaur, "The effects of varying viscosity and thermal conductivity on steady free convective flow and heat transfer along an isothermal vertical plate in presence of heat sink," Journal of Applied Fluid Mechanics, vol. 2, no.1, pp. 23-28, 2009. doi: https://www.researchgate.net/publication/26579367

[16] M. Nakamura, and T. Sawada, "Numerical study on the flow of a non-Newtonian fluid through an axisymmetric stenosis," Journal of Biomechanical Engineering, Vol. 110, no. 137, pp. 137-143,1988. doi: http://dx.doi.org/10.1115/1.3108418

[17] A. Neeraja, R. R. Devi, B. Devika, V. N. Radhika, and M. K. Murthy, "Effects of viscous dissipation and convective boundary conditions on magnetohydrodynamics flow of casson liquid over a deformable porous channel," Results in Engineering, vol. 4, pp. 100040, 2019. doi: https://doi.org/10.1016/j.rineng.2019.100040

[18] P.R. Nachtsheim,and P. Swigert, "Satisfaction of the asymptotic boundary conditions in numerical solution of the systems of non-linear equations of boundary layer type," Ph.D. Thesis, National Aeronautics and Space Administration, vol. 3004, 1965.

[19] J.C. Misra, and A. Sinha, "Effect of thermal radiation on MHD flow of blood and heat transfer in a permeable capillary in stretching motion," Heat Mass Transfer, vol. 49, pp. 617-628, 2013. doi: https://doi.org/10.1007/s00231-012-1107-6

[20] S. Pramanik, "Casson fluid flow and heat transfer past an exponentially porous stretching surface in presence of thermal radiation," Ain shams engineering journal, vol. 5, no. 1, pp. 205-212, 2014. doi: https://doi.org/10.1016/j.asej.2013.05.003